

# Impulse radio ultrawideband pulse shaper based on a programmable photonic chip frequency discriminator

David Marpaung,<sup>1,\*</sup> Ludovic Chevalier,<sup>2</sup> Maurizio Burla<sup>1</sup> and Chris Roeloffzen<sup>1</sup>

<sup>1</sup>Telecommunication Engineering group, University of Twente, PO Box 217, Enschede.7500 AE, the Netherlands

<sup>2</sup>ENSIL, Electronics and Telecommunications, 16 rue Atlantis, 87068, Limoges, France

\*[d.a.i.marpaung@ewi.utwente.nl](mailto:d.a.i.marpaung@ewi.utwente.nl)

**Abstract:** We report and experimentally demonstrate the generation of impulse radio ultrawideband (UWB) pulses using a photonic chip frequency discriminator. The discriminator consists of three add-drop optical ring resonators (ORRs) which are fully programmable using thermo-optical tuning. This discriminator chip in combination with a phase modulator forms a temporal differentiator where phase modulation is converted to intensity modulation (PM-IM conversion). By means of tailoring the discriminator response using either the individual or the cascade of drop and through responses of the ORRs, first-order or second-order temporal differentiations are obtained. Using this principle, the generation of UWB monocycle, doublet and modified doublet pulses are demonstrated. The use of this CMOS-compatible discriminator is promising for the realization of a compact and low cost UWB transmitter.

©2011 Optical Society of America

**OCIS codes:** (060.2360) Fiber optics links and subsystems; (060.5060) Phase modulation; (060.5625) Radio frequency photonics; (070.6020) Continuous optical signal processing; (130.3120) Integrated optics devices; (350.4010) Microwaves.

---

## References and links

1. J. Capmany and D. Novak, "Microwave photonics combines two worlds," *Nat. Photonics* **1**(6), 319–330 (2007).
2. M. H. Khan, H. Shen, Y. Xuan, L. Zhao, S. Xiao, D. E. Leaird, A. M. Wiener, and M. Qi, "Ultrabroadbandwidth arbitrary radiofrequency waveform generation with a silicon photonic chip-based spectral shaper," *Nat. Photonics* **4**(2), 117–122 (2010).
3. J. Yao, F. Zheng, and Q. Wang, "Photonic generation of ultrawideband signals," *J. Lightwave Technol.* **25**(11), 3219–3235 (2007).
4. J. Azaña, "Ultrafast analog all-optical signal processors based on fiber-grating devices," *IEEE Photonics J.* **2**(3), 359–386 (2010).
5. M. Ferrera, Y. Park, L. Razzari, B. E. Little, S. T. Chu, R. Morandotti, D. J. Moss, and J. Azaña, "On-chip CMOS-compatible all-optical integrator," *Nat Commun.* **1**(3), 29 (2010).
6. F. Liu, T. Wang, L. Qiang, T. Ye, Z. Zhang, M. Qiu, and Y. Su, "Compact optical temporal differentiator based on silicon microring resonator," *Opt. Express* **16**(20), 15880–15886 (2008).
7. Y. Park, M. H. Asghari, R. Helsten, and J. Azaña, "Implementation of broadband microwave arbitrary-order time differential operators using a reconfigurable incoherent photonic processor," *IEEE Photonics J.* **2**(6), 1040–1050 (2010).
8. C. Wang, F. Zeng, and J. Yao, "All-fiber ultrawideband pulse generation based on spectral shaping and dispersion-induced frequency-to-time conversion," *IEEE Photon. Technol. Lett.* **19**(3), 137–139 (2007).
9. M. Abtahi, J. Magné, M. Mirshafiei, L. A. Rusch, and S. LaRochelle, "Generation of power efficient FCC-compliant UWB waveforms using FBGs: analysis and experiment," *J. Lightwave Technol.* **26**(5), 628–635 (2008).
10. Q. Wang and J. Yao, "UWB doublet generation using nonlinearly-biased electro-optic intensity modulator," *Electron. Lett.* **42**(22), 1304–1306 (2006).
11. S. T. Abraha, C. M. Okonkwo, E. Tangdionga, and A. M. J. Koonen, "Power-efficient impulse radio ultrawideband pulse generator based on the linear sum of modified doublet pulses," *Opt. Lett.* **36**(12), 2363–2365 (2011).

12. V. Torres-Company, K. Prince, and I. T. Monroy, "Fiber transmission and generation of ultrawideband pulses by direct current modulation of semiconductor lasers and chirp-to-intensity conversion," *Opt. Lett.* **33**(3), 222–224 (2008).
13. X. Yu, T. Braidwood Gibbon, M. Pawlik, S. Blaaberg, and I. Tafur Monroy, "A photonic ultra-wideband pulse generator based on relaxation oscillations of a semiconductor laser," *Opt. Express* **17**(12), 9680–9687 (2009).
14. Q. Wang, F. Zeng, S. Blais, and J. Yao, "Optical ultrawideband monocycle pulse generation based on cross-gain modulation in a semiconductor optical amplifier," *Opt. Lett.* **31**(21), 3083–3085 (2006).
15. Q. Wang and J. P. Yao, "Switchable optical UWB monocycle and doublet generation using a reconfigurable photonic microwave delay-line filter," *Opt. Express* **15**(22), 14667–14672 (2007).
16. J. Li, S. Fu, K. Xu, J. Wu, J. Lin, M. Tang, and P. Shum, "Photonic ultrawideband monocycle pulse generation using a single electro-optic modulator," *Opt. Lett.* **33**(3), 288–290 (2008).
17. M. Bolea, J. Mora, B. Ortega, and J. Capmany, "Optical UWB pulse generator using an  $N$  tap microwave photonic filter and phase inversion adaptable to different pulse modulation formats," *Opt. Express* **17**(7), 5023–5032 (2009).
18. F. Zeng and J. Yao, "An approach to ultrawideband pulse generation and distribution over optical fiber," *IEEE Photon. Technol. Lett.* **18**(7), 823–825 (2006).
19. F. Zeng and J. P. Yao, "Ultrawideband impulse radio signal generation using a high-speed electro-optic phase modulator and a fiber-Bragg-grating-based frequency discriminator," *IEEE Photon. Technol. Lett.* **18**(19), 2062–2064 (2006).
20. J. Li, K. Xu, S. Fu, M. Tang, P. Shum, J. Wu, and J. Lin, "Photonic polarity-switchable ultra wideband pulse generation using a tunable Sagnac interferometer comb filter," *IEEE Photon. Technol. Lett.* **20**(15), 1320–1322 (2008).
21. S. Pan and J. Yao, "Switchable UWB pulse generation using a phase modulator and a reconfigurable asymmetric Mach-Zehnder interferometer," *Opt. Lett.* **34**(2), 160–162 (2009).
22. Y. Dai, J. Du, X. Fu, G. K. P. Lei, and C. Shu, "Ultrawideband monocycle pulse generation based on delayed interference of  $\pi/2$  phase-shift keying signal," *Opt. Lett.* **36**(14), 2695–2697 (2011).
23. F. Liu, T. Wang, Z. Zhang, M. Qiu, and Y. Su, "On-chip photonic generation of ultra-wideband monocycle pulses," *Electron. Lett.* **45**(24), 1247–1248 (2009).
24. J. Dong, X. Zhang, J. Xu, D. Huang, S. Fu, and P. Shum, "Ultrawideband monocycle generation using cross-phase modulation in a semiconductor optical amplifier," *Opt. Lett.* **32**(10), 1223–1225 (2007).
25. E. Zhou, X. Xu, K. S. Lui, and K. K. Y. Wong, "A power-efficient ultra-wideband pulse generator based on multiple PM-IM conversions," *IEEE Photon. Technol. Lett.* **22**(14), 1063–1065 (2010).
26. I. Gasulla, J. Lloret, J. Sancho, S. Sales, and J. Capmany, "Recent breakthrough in microwave photonics," *IEEE Photonics J.* **3**(2), 311–315 (2011).
27. P. Samadi, L. R. Chen, C. Callender, P. Dumais, S. Jacob, and D. Celo, "RF arbitrary waveform generation using tunable planar lightwave circuit," *Opt. Commun.* **284**(15), 3737–3741 (2011).
28. L. Zhuang, C. G. H. Roeloffzen, A. Meijerink, M. Burla, D. A. I. Marpaung, A. Leinse, M. Hoekman, R. G. Heideman, and W. van Etten, "Novel ring resonator-based integrated photonic beamformer for broadband phased array receive antennas—Part II: Experimental prototype," *J. Lightwave Technol.* **28**(1), 19–31 (2010).
29. N. N. Feng, P. Dong, D. Feng, W. Qian, H. Liang, D. C. Lee, J. B. Luff, A. Agarwal, T. Banwell, R. Menendez, P. Toliver, T. K. Woodward, and M. Asghari, "Thermally-efficient reconfigurable narrowband RF-photonic filter," *Opt. Express* **18**(24), 24648–24653 (2010).
30. S. Ibrahim, N. K. Fontaine, S. S. Djordjevic, B. Guan, T. Su, S. Cheung, R. P. Scott, A. T. Pomerene, L. L. Seaford, C. M. Hill, S. Danziger, Z. Ding, K. Okamoto, and S. J. B. Yoo, "Demonstration of a fast-reconfigurable silicon CMOS optical lattice filter," *Opt. Express* **19**(14), 13245–13256 (2011).
31. D. Marpaung, C. Roeloffzen, A. Leinse, and M. Hoekman, "A photonic chip based frequency discriminator for a high performance microwave photonic link," *Opt. Express* **18**(26), 27359–27370 (2010).
32. H. Nikoosar and M. Prasad, "Introduction to ultra wideband for wireless communications," in *Springer Science and Business Media* (Springer-Verlag, New York, 2009).
33. L. Zhuang, D. Marpaung, M. Burla, W. Beeker, A. Leinse, and C. G. H. Roeloffzen, "Low-loss, high-index-contrast  $\text{Si}_3\text{N}_4/\text{SiO}_2$  optical waveguides for optical delay lines in microwave photonics signal processing," *Opt. Express* **19**(23), 23162–23170 (2011).
34. J. F. Bauters, M. J. R. Heck, D. John, M.-C. Tien, W. Li, J. S. Barton, D. J. Blumenthal, A. Leinse, and R. G. Heideman, "Ultra-low loss single mode silicon nitride waveguides with 0.7 dB/m propagation loss," in *37th European Conference and Exposition on Optical Communications*, OSA Technical Digest (CD) (Optical Society of America, 2011), paper Th.12.LaSaleve.3.

## 1. Introduction

Microwave photonics (MWP) techniques for the generation and processing of RF signals have enjoyed a surge of interests in the last few years. Generation of arbitrary microwave and RF waveforms [1–3] and fundamental RF signal processing techniques such as differentiation and integration [4–7] using photonic devices and systems have recently been reported. These functionalities have exploited the advantage of unprecedented bandwidth of photonics. One

application that benefits from these functionalities is the ultrawideband (UWB) over fiber technology. In this approach UWB signals are generated and later on distributed in the optical domain to increase the reach of the UWB transmission, similar to the more general concept of radio over fiber. In the last five years numerous techniques have been proposed for the so-called photonic generation of impulse-radio UWB (IR-UWB) pulses [3,8–25]. The generated pulses are usually the variants of Gaussian monocycles, doublets or in some occasion higher-order derivatives of the basic Gaussian pulses. These techniques usually aim at generating the pulses which power spectral densities (PSD) satisfy the regulation (i.e. spectral mask) specified by the U.S. Federal Communications Commission (FCC) for indoor UWB systems.

Different techniques that have been proposed for IR-UWB pulses generation include spectral shaping combined with frequency-to-time mapping [8,9], nonlinear biasing of a Mach-Zehnder modulator (MZM) [10,11], and direct modulation of a semiconductor laser by exploiting the frequency chirp [12] or the relaxation oscillation [13]. The most popular techniques to generate the UWB pulses, however, are based on two principles. The first approach is to use MWP delay-line filter to achieve either spectral filtering of the Gaussian input in the frequency domain or to approximate  $n$ th-order derivatives of the Gaussian input pulse with the  $n$ th-order differences [7,14–18]. In the second approach, phase modulation-to-intensity modulation (PM-IM) conversion is used to achieve temporal differentiations (in most cases first-order derivatives, i.e. monocycles) of the input Gaussian pulse [19–25].

On the other hand, nowadays we have seen a growing trend to demonstrate various MWP functionalities with on-chip integrated photonic approach [26]. Functionalities like integrator [5], differentiator [6], arbitrary waveform generation [27], beam forming [28], RF filtering [29,30] and MWP link [31] have been demonstrated in integrated photonic form very recently. Keeping up with these approaches, we recently reported a CMOS-compatible photonic chip frequency discriminator [31] consisting of optical ring resonators (ORRs) in an add-drop configuration. These ORRs are fully programmable using thermo-optical tuning mechanism. The discriminator chip was initially implemented in a phase-modulated MWP link [31] to perform a PM-IM conversion, leading to a high dynamic range analog photonic link with a simple direct detection scheme instead of the complex coherent detection.

In this paper we use the photonic chip discriminator reported in [31] to perform the PM-IM conversion necessary in a photonic IR-UWB generator. We experimentally demonstrate the generation of Gaussian monocycles, doublets and the modified doublets [11] that comply with the FCC-regulation for indoor UWB transmission [32]. The approach of using a ring resonator as frequency discriminator and UWB pulses generation has previously been reported by Liu et al. [6,23]. In these reported works, the PM-IM conversion was achieved using the linear region of the power response of an all-pass microring resonator and the generated pulses were limited to Gaussian monocycles. In this paper we use the through or drop responses of an ORR to generate monocycle pulses and the cascade of different ORR responses to generate the doublets and the modified doublets. To the best of our knowledge, this is the very first demonstration of IR-UWB pulses generation, beyond the simple monocycles using an integrated photonic chip. As explicitly stated in several previously reported works [11,20–22], the approach of IR-UWB pulses generation using an integrated photonic chip instead of discrete components is highly desirable.

## 2. Theoretical analysis of UWB generation

A typical signal commonly considered as the basis function in IR-UWB transmission is the Gaussian pulse expressed as [32]

$$x(t) = \frac{A}{(2\pi)^{1/2} \sigma} \exp\left(-\frac{t^2}{2\sigma^2}\right) \quad (1)$$

where  $A$  and  $\sigma$  are the amplitude and the spread factor of the Gaussian pulse, respectively. As mentioned earlier, most of the approaches reported for photonic generation of IR-UWB pulses are aiming at the creation of higher-order derivatives of the pulse in Eq. (1) in order to reduce the low-frequency components in the pulse and to comply with the FCC regulation. The normalized power spectral density (PSD) of the  $n$ th-order derivatives of the pulse in Eq. (1) can be expressed as [32]

$$S_n(\omega) = \frac{(\omega\sigma)^{2n} \exp(-(\omega\sigma)^2)}{n^n \exp(-n)} \quad (2)$$

where  $\omega = 2\pi f$  is the angular frequency and  $n$  is the order of derivation. Substituting  $n = 0, 1$  or  $2$  to Eq. (2) will result in the PSD of the Gaussian pulse, monocycle or doublet, respectively. The PSDs of these pulses, with  $\sigma = 50$  ps are plotted in decibels in Fig. 1a. As seen in this figure, the monocycle and the doublet can be obtained by means of filtering the spectrum of the Gaussian pulse. In this case, the  $n$ th-order derivative PSD can be written as

$$S_n(\omega) = |H_n(\omega)|^2 S_0(\omega) \quad (3)$$

where  $S_0(\omega)$  is the PSD of the Gaussian input and  $H_n(\omega)$  is the transfer function of the filter used to generate the  $n$ th-order derivative. The squared magnitude of the transfer functions calculated from Eqs. (2) and (3) are plotted in Fig. 1b. It can be seen that the filter attenuates the low frequency components of the input Gaussian pulse. For this reason, the resulting higher-order derivative pulses are more suited for transmission with antennas and comply better with the FCC regulation [32]. Thus, in order to generate the monocycle or the doublet one must synthesize the magnitude responses in Fig. 1b. This filtering technique for photonic IR-UWB generation has been investigated in the past [3,7,14–18]. In this case, the approach essentially reduces to synthesizing a microwave photonic filter (MPF) with an electrical transfer function approximating the filter responses in Fig. 1b or even more complicated responses [17]. In this work we will demonstrate that the PM-IM conversion using the frequency discriminator chip constitutes an MPF with a transfer function that can be programmed to generate the monocycle, doublet and potentially more complex responses.

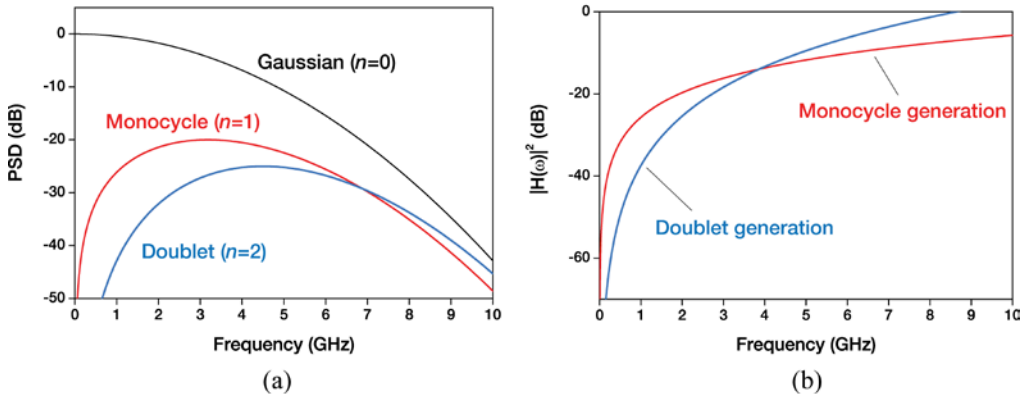


Fig. 1. (a) The power spectral densities (PSDs) of the Gaussian, monocycle and doublet pulses (Eq. (2)) for  $\sigma = 50$  ps. (b) Squared magnitude of the filter response that shapes the spectrum of the input Gaussian pulse into the spectrum of the monocycle or the doublet.

### 3. The photonic chip frequency discriminator

The schematic of the photonic chip discriminator used in this work is shown in Fig. 2a. The chip consists of five add-drop ring resonators. However, in this work only three of the rings

(Rings 1-3) are used while Rings 4 and 5 are tuned out of resonance to show an all-pass filter response and hence do not play any role in the experiments. The ORRs have a free spectral range of 21.5 GHz and they are fully-reconfigurable in terms of resonance frequency and quality factor using thermo-optical tuning mechanism. The tuning speed to fully reconfigure the ORR response is in the order of 0.5 ms. During the experiments the chip is temperature stabilized to maintain the desired response. For the ease of the measurements, the chip has been packaged, where electrical connections to a pair of PCBs have been established (for tuning purposes) and fiber array units have been connected to the optical inputs and outputs. The measured fiber to-chip coupling loss is 12.5 dB/facet. The loss is mainly attributed to the absence of spot size converters at the chip facets [31]. The photograph of the packaged frequency discriminator is shown in Fig. 2b. The details of the chip fabrication (waveguide technology, ORR specifications) and characterization (waveguide propagation loss, fiber-to-chip coupling loss) have been reported in [31].

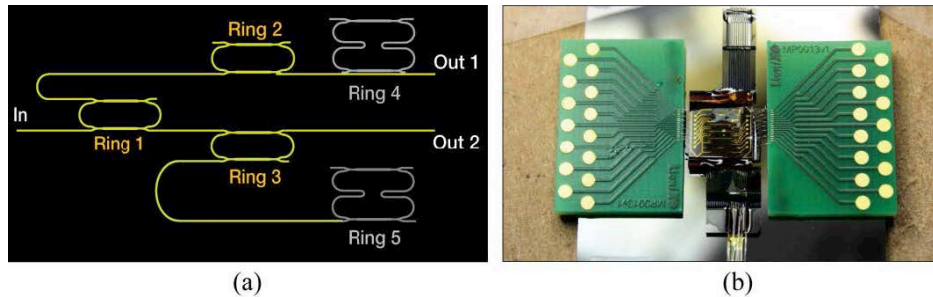


Fig. 2. The photonic chip frequency discriminator used in this work. (a) Chip schematic. Three ORRs are used to simultaneously generate the IR-UWB pulses from Out 1 and Out 2. (b) The packaged photonic chip with fiber array units and wirebonded PCBs (from [31]).

The ORRs in the chip are arranged such that two outputs can simultaneously be used in the experiments. At Out 1 one can observe three different responses depending on the programmed settings, namely the drop response of Ring 1, the through response of Ring 2 or the cascade of these responses. Similarly, at Out 2, the individual through responses of Ring 1 and Ring 3 as well as the cascade of these responses can be obtained. The programmability of the output responses of the chip is very high since each ORR can independently be configured in terms of resonance frequency and quality factor (Q-factor). The chip is then programmed to synthesize the output responses that lead to the generation of IR-UWB pulses.

#### 4. Experiments

The schematic of the measurement setup is shown in Fig. 3. The light from a high power DFB laser (EM4 Inc.) is phase modulated in a 10-GHz phase modulator (Covega Mach-10) with electrical Gaussian pulses generated by a pulse pattern generator (PPG) (Anritsu MP17633). The PPG is driven at a rate of 4 Gb/s with a fixed pattern of one “1” per 64 bits which are equivalent to a Gaussian pulse train with a repetition rate of 62.5 MHz. This relatively low rate was chosen such that output pulse from the system can still be measured using an oscilloscope (Agilent 54850) with a maximum frequency 4 GHz (an oscilloscope with a higher frequency range was not available during the experiments). In this case the theoretical Gaussian pulse full width at half-maximum (FWHM) is about 250 ps. Later on, when the compliance with the FCC spectral mask of the shaped pulse is investigated, the PPG was driven with repetition rate of 12.5 Gb/s with a pattern of one “1” per 64 bits. In this case the Gaussian pulse FWHM is 80 ps. In all cases the peak-to-peak amplitude ( $V_{pp}$ ) of these pulses is set to 2.5 V. The phase modulated signal is then transferred into intensity modulation in the discriminator photonic chip. To overcome the loss in the optical chip a pair of EDFAs is used at the outputs of the discriminator prior to the photodetectors. Here we use a 10 GHz balanced

photodetector (BPD, DSC 710) where the inputs are addressed one at a time. To measure the spectrum of the shaped pulses an RF spectrum analyzer (RFSA, Agilent MXA N9020A) is used.

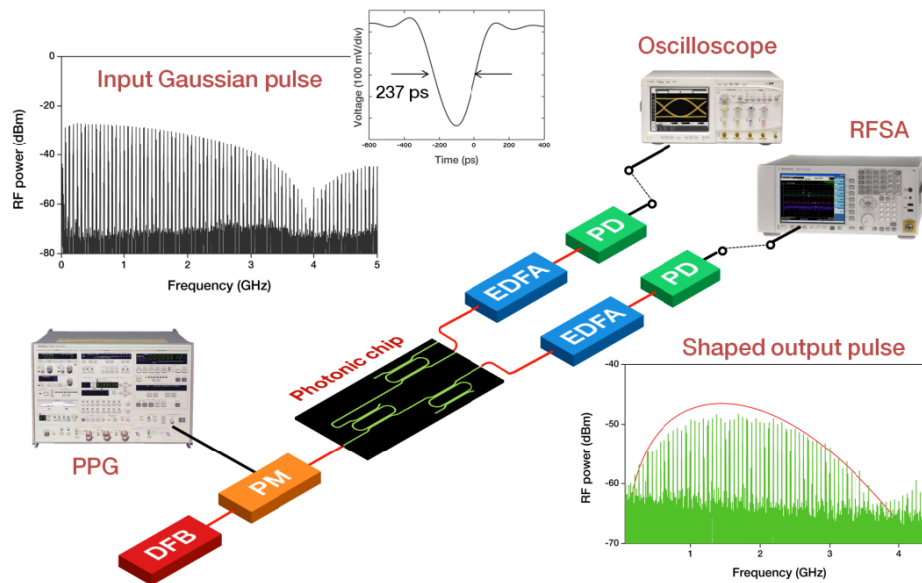


Fig. 3. Schematic of the measurement setup used to demonstrate the pulse shaping. The discriminator chip is configured to shape the Gaussian pulses modulated onto the phase of the optical carrier into a monocycle or a doublet. To overcome the fiber-to-chip coupling loss a pair of EDFAs is placed at the chip output. DFB: distributed feedback laser, PPG: pulse pattern generator, PM: phase modulator, PD: photodetector, RFSA: RF spectrum analyzer.

## 5. Experiment results and discussions

### 5.1 Monocycle generation with one ORR

To generate monocycle pulses the photonic chip is programmed such that only one ORR is in resonance (in this case Ring 1 of Fig. 2a). The other ORRs are tuned out of resonance. We select the through response of Ring 1 observed at Out 2 of the chip (Fig. 1) to perform the PM-IM conversion. In principle, the drop response (from Out 1) should also yield similar results. A similar technique as reported in [31] has been used to characterize the static (i.e. without modulation) response of the ORR. The result is depicted in Fig. 4a, which clearly shows the notch filter behavior of the ORR through response. This static characteristic will be used to set the laser wavelength for operation in the desired region of the filter response. Next, the laser light is phase modulated with a Gaussian electrical pulse train as described in the previous section. The waveform and the PSD of the input Gaussian pulse are depicted in the inset of Fig. 3. The FWHM of the Gaussian pulse is measured to be 237 ps and the spectral content reaches to 4 GHz. To achieve PM-IM conversion the laser wavelength is aligned to each of the linear slopes (positive and negative slopes in Fig. 4a) of the through response. Depending on the slope of the PM-IM conversion, Gaussian monocycles with opposite polarities are generated. The measured waveforms of these monocycles are shown in Fig. 4b. The PSD of the positive polarity monocycle is then measured and the result is shown in Fig. 4c. The measured response is compared to the theoretical PSD of a monocycle obtained from Eq. (2) by substituting  $n = 1$  and  $\sigma = 110$  ps. A proper attenuation factor has been chosen to have a good fit. The measured PSD shows a good agreement with the theoretical response. Next, we measure the electrical transfer function from the input of the phase modulator to the

output of the photodetector using a vector network analyzer (Agilent PNA N5230A). This constitutes a squared magnitude response of a microwave photonic filter (MPF) as suggested in Eq. (3). The measured result is compared to the calculated MPF response for monocycle generation (Eq. (3) and Fig. 1b). These results are shown in Fig. 4d. The measurement and the calculated response show a similar trend and a good match at lower frequencies (lower than 3 GHz). Deviations are observed at higher frequencies which might come from the limited range of the linear region of the ORR response. As analyzed in [31] this is directly limited by the waveguide propagation loss in the optical chip (1.2 dB/cm at 1550 nm). However, a much lower propagation loss of below 0.1 dB/cm can already be achieved using the same waveguide technology as the one used in our photonic chip [33].

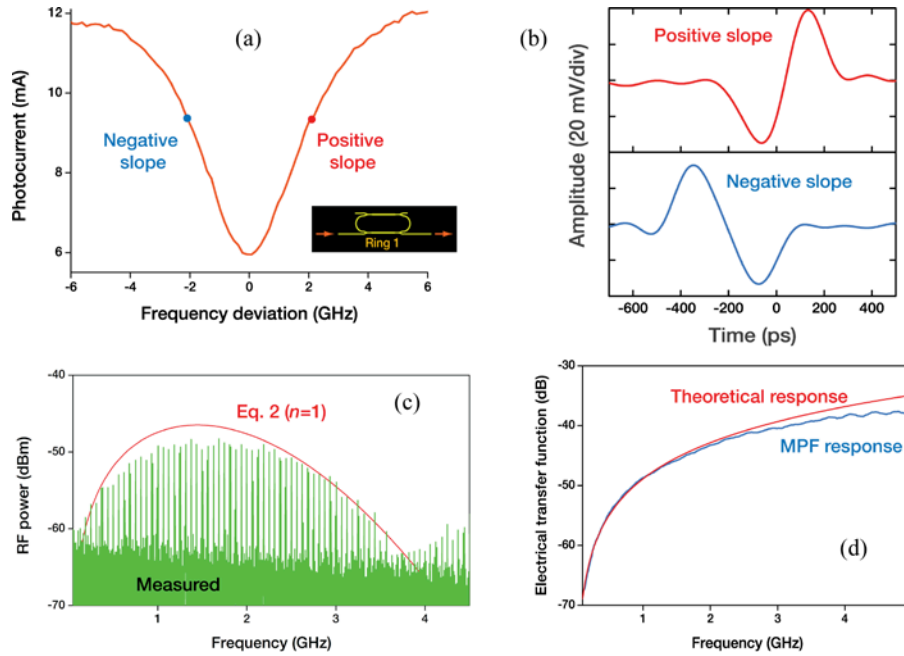


Fig. 4. Measurement results on the monocycle generation with one ORR. (a) Measured Ring 1 through response. (b) Waveforms of the generated monocycles. (c) Power spectral density of the positive polarity monocycle. (d) Comparison of the theoretical and the measured transfer function of the microwave photonic filter synthesized for the monocycle generation.

Besides the MPF theory, a time domain approach can also be used to understand the process of monocycle generation with this frequency discriminator chip. As previously reported [6,23], PM-IM conversion with a ring resonator can be regarded as temporal differentiation of the input electrical pulse. This is illustrated in Fig. 5a. Since the phase modulator is driven with a Gaussian pulse, the instantaneous phase of the optical signal,  $\phi(t)$ , resembles a Gaussian shape. The instantaneous frequency, being the first-order derivative of  $\phi(t)$ , takes the monocycle function. This instantaneous change in frequency is linearly transferred into instantaneous change in optical power via the linear response of the ORR which essentially is a frequency discriminator. This results in a monocycle electrical pulse after the photodetection process. As explained before, this behavior can be explained in the frequency domain representation as a simple filtering of the input Gaussian PSD,  $S_0(\omega)$ , to produce the PSD of the monocycle,  $S_1(\omega)$  at the output. This is illustrated in Fig. 5b.

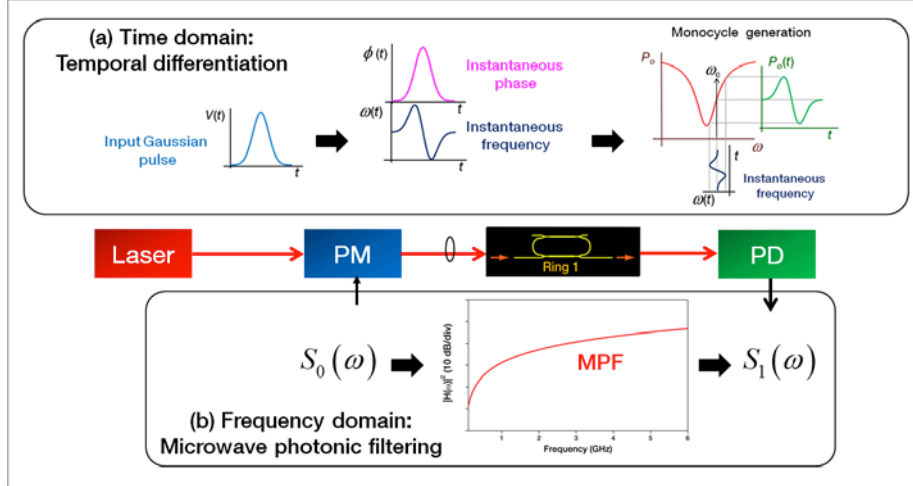


Fig. 5. Two ways to explain the monocycle generation using the ORR frequency discriminator. (a) Time domain approach where the instantaneous frequency change of the optical carrier is linearly transferred to the intensity modulation via linear frequency discrimination. (b) Frequency domain approach, where the monocycle is generated via MPF spectral filtering of the input Gaussian pulse.

### 5.2 Doublet and modified doublet generation with cascaded ORRs

To generate Gaussian doublets the photonic chip is programmed such that two ORRs, Ring 1 and Ring 3, are in resonance. The cascade of two through responses of these ORRs is observed at Out 2. By means of tuning the phase shifters on the rings [31], the resonance frequency of Ring 3 can be brought closer to the resonance frequency of Ring 1. The measured cascade response is shown in Fig. 6a together with the simulated response as well as the individual through responses of Ring 1 and Ring 3. Next, the laser wavelength is tuned to the position indicated also in Fig. 6a. The electrical signal from Out 2 after photodetection process is a Gaussian doublet with a waveform shown in Fig. 6b. The width of the pulse is 162 ps. The measured PSD of this pulse is shown in Fig. 6c. The measured spectrum is compared with the calculated doublet spectrum from Eq. (2), substituting  $n = 2$  and  $\sigma = 110$  ps (shown as the envelope in Fig. 6c). The measured MPF electrical transfer function of the system programmed for double generation is depicted in Fig. 6d. The measured values (thick line) are compared with the calculated response (thin line). As observed in the monocycle generation, a deviation is occurred at higher frequencies (beyond 3 GHz). This might be attributed to the limited frequency range of the response in Fig. 6a usable for the doublet generation.

In previously reported investigations of photonic generation of IR-UWB pulses, compliance with the FCC spectral mask is often emphasized. In this case it is desired to fill the spectral mask efficiently without violating it. Recently, Abraha et al. [11] reported a scheme where an FCC compliant pulse is generated using a linear combination of modified doublet pulses. The modified doublet is a doublet variant of which the amplitude ratio between its positive and negative part of the doublet pulse is slightly modified [11]. In the frequency domain, this type of pulses can be distinguished from a conventional doublet by a notch in the lower frequency region of its PSD. Theoretically, the PSD of the modified doublet can be expressed as

$$S_{\text{mod}}(\omega) = \left( (1-k)\sigma + k\sigma^3\omega^2 \right)^2 \exp\left(-(\omega\sigma)^2\right) \quad (4)$$

where  $k$  is an arbitrary scaling parameter. In case of  $k = 1$  the pulse becomes a conventional doublet.

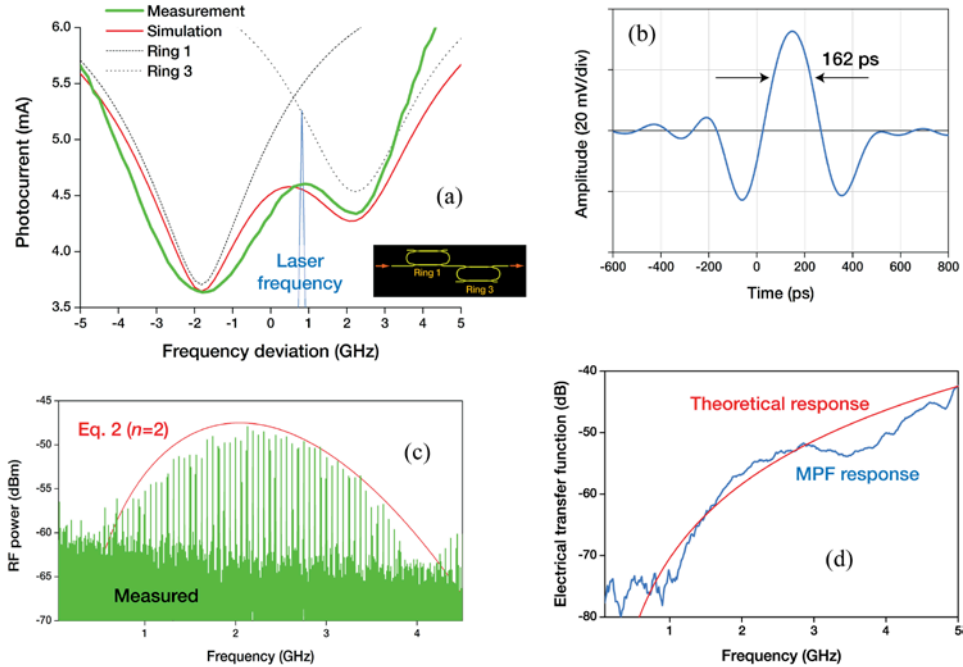


Fig. 6. Measurement results on the doublet generation with a cascade of two ORRs. (a) Measured Ring 1 and Ring 3 through responses depicted together with simulation results. (b) Waveforms of the generated doublet. (c) Power spectral density of the generated doublet compared with the theoretical response. (d) Comparison of the theoretical and the measured transfer function of the microwave photonic filter synthesized for the doublet generation.

In order to demonstrate the generation of a modified doublet and to check the spectral compliance with the FCC indoor mask a higher bit rate (12.5 Gb/s) from the PPG is used. The chip is then carefully tuned while observing the output PSD of the generated pulses. This procedure is equivalent to adjusting the scaling parameter,  $k$ , such that the notch in the pulse PSD is aligned with the notch in the FCC mask that corresponds to the GPS frequency band (0.96-1.61 GHz) [32]. The measured PSD is depicted in Fig. 7, together with the calculated PSD from Eq. (4). The best fit of the measured and the calculated PSDs is obtained with  $k = 1.24$  and  $\sigma = 50$  ps. As can be seen from the figure, the resulting pulse does not fully comply with the FCC regulation. This is expected since theoretically the modified doublet by itself

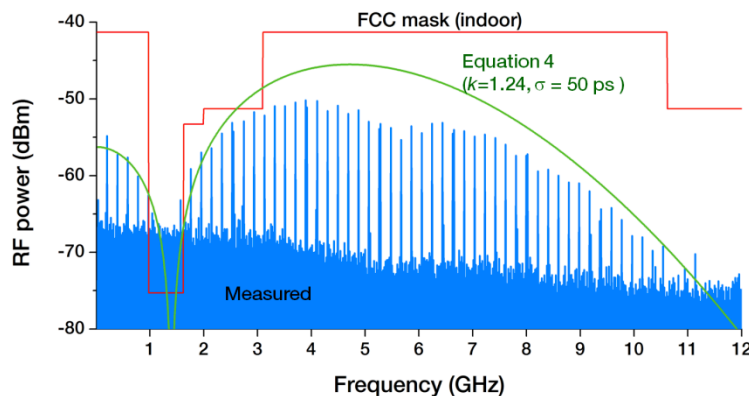


Fig. 7. The power spectrum of a modified doublet pulse generated from the cascade of through responses of two ORRs. The envelope is calculated using Eq. (4).

does not fit the FCC mask. The linear combination of two of such pulses with different polarity and a time delay between them will eventually satisfy the FCC regulation [11]. But to the best of our knowledge, this is the very first demonstration of a modified doublet generation using an integrated photonic chip approach

### 5.3 Simultaneous generation of two modified doublets

So far we have demonstrated the generation of a wide variety of UWB pulses from one output of the photonic chip (Out 2). The other output that consists of the drop response of Ring 1 and the through response of Ring 2 can also be programmed to generate UWB pulses. In fact, the two outputs can be programmed to simultaneously yield UWB pulses. This is particularly interesting since it has been demonstrated that FCC compliant pulses can be generated by means of a linear combination of two time-delayed UWB pulses, like the modified doublets [11] or asymmetric monocycles [25]. Thus, it is desirable to have a pair of UWB pulses from the same system that can later on be delayed and linearly combined to create more complex pulses. For the sake of demonstration, we programmed the photonic chip such that both outputs simultaneously produce two modified doublets.

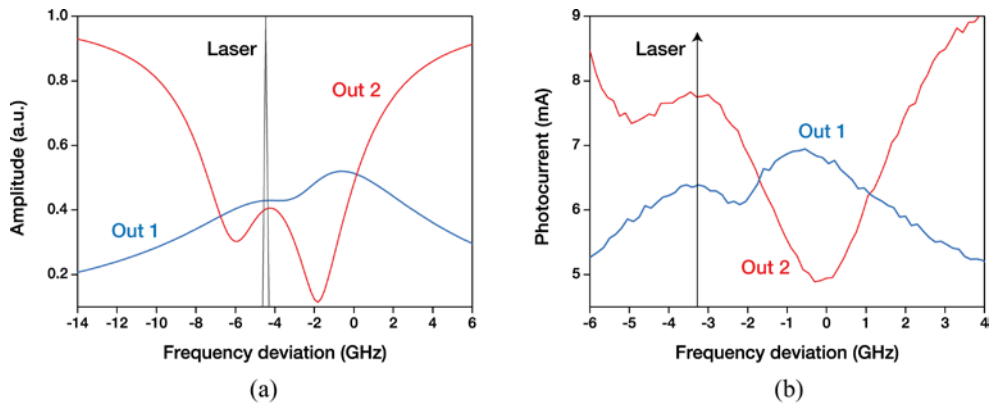


Fig. 8. The photonic chip discriminator response used for simultaneous generation of two modified doublets from Out 1 and Out 2. (a) Simulated responses. (b) Measured responses. The relative position of the laser frequency is indicated by the arrow.

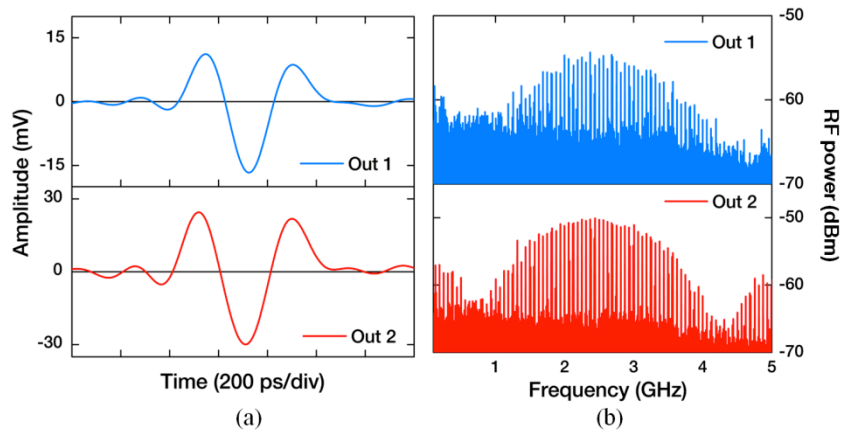


Fig. 9. Measurement results on the simultaneous generation of two modified doublets from Out 1 and Out 2. (a) Waveforms of the generated pulses. (b) Power spectral density of the generated modified doublets.

The two outputs are configured to achieve the simulated responses in Fig. 8a. The measured responses are depicted in Fig. 8b. The Gaussian pulse train with the rate of 4 Gb/s has been used for the experiment. The measured time waveforms of the generated modified doublets are shown in Fig. 9a. The pulse generated from Out 1 has smaller amplitude compared to Out 2. The measured PSDs of the two pulses are shown in Fig. 9b. The notches in the lower frequency region of the PSDs clearly indicate the generation of modified doublets. This feature is less apparent for the pulse generated from Out 1 because of a poorer signal-to-noise ratio relative to Out 2.

As has been previously demonstrated, these two modified doublets can then be mutually delayed and linearly combined to create a more complex (and FCC compliant) pulse. It is customary to generate this mutual delay with a length difference of two optical fibers [11]. It is very interesting however, to combine the UWB generation technique reported in this work together with on-chip delay generation. This however requires ultra-low loss optical waveguides as delay lines. Recently, such a delay line with a propagation loss as low as 0.7 dB/m has been demonstrated using a high-index-contrast stoichiometric silicon nitride waveguides [34]. Combined with the work presented here, such CMOS-compatible delay lines will be very relevant for low cost and compact photonic IR-UWB transmitters.

## 6. Conclusions

The generation of IR-UWB pulses using a photonic chip frequency discriminator has been reported. The high degree of programmability of the chip allows the generation of a wide-variety of pulses, such as opposite polarity monocycles, conventional and modified doublets. Analysis of the generation process has been presented based on the time domain (temporal differentiation) and frequency domain (microwave photonic filtering) approaches. We believe this is the first time the generation of UWB pulses beyond the monocycles is demonstrated with integrated photonic chip. The reported work is very relevant for the development of low cost photonic IR-UWB pulse shaper and transmitter. The possibility to implement this pulse generation technique to be adaptable for various modulation formats will be investigated.

## Acknowledgments

The research described in this paper is partly funded by the European Commission in the 7th Framework Program. The SANDRA project is a Large Scale Integrating Project for the FP7 Topic AAT.2008.4.4.2 (Integrated approach to network centric aircraft communications for global aircraft operations). This work is also partially funded by the MEMPHIS project supported by the Smart Mix Programme of the Dutch Ministry of Economic Affairs and the Ministry of Education, Culture and Science. The authors would like to thank Marcel Hoekman and Arne Leinse from LioniX BV for the fabrication of the photonic chip discriminator and Henk de Vries for providing the pulse pattern generator.